PHYSICAL REVIEW B **73**, 220401(R) (2006)

Inversion-symmetry breaking in the noncollinear magnetic phase of the triangular-lattice antiferromagnet $CuFeO_2$

T. Kimura,[1,2] J. C. Lashley,[1] and A. P. Ramirez[2]
[1]*Los Alamos National Laboratories, Los Alamos, New Mexico 87545, USA*
[2]*Bell Laboratories, Lucent Technologies, 600 Mountain Avenue, Murray Hill, New Jersey 07974, USA*
(Received 9 May 2006; published 12 June 2006)

Magnetoelectric and magnetoelastic phenomena have been investigated on a frustrated triangular antiferromagnetic lattice in $CuFeO_2$. Inversion-symmetry breaking, manifested as a finite electric polarization, was observed in noncollinear (helical) magnetic phases and not in collinear magnetic phases. This result demonstrates that the noncollinear spin structure plays an important role in inducing electric polarization. Based on these results we suggest that frustrated magnets (often favoring noncollinear configurations) are favorable candidates for a new class of magnetoelectric materials.

DOI: 10.1103/PhysRevB.73.220401 PACS number(s): 75.30.Kz, 64.70.Rh, 75.80.+q

Ordered and unordered ground states in geometrically frustrated magnetic systems often lead to exotic properties such as spin liquid, spin ice, multicritical phenomena, and noncollinear ordering.[1,2] Among such states are long-wavelength magnetic structures that arise from competing interactions. Similarly, some multiferroic materials[3,4] show long-wavelength magnetic structures in addition to unusually strong couplings between magnetism and ferroelectricity.[5–8] For example, $TbMnO_3$ with long-wavelength magnetic structure exhibits a ferroelectric order as well as a gigantic magnetoelectric effect.[7] A recent neutron diffraction measurement on $TbMnO_3$ revealed that the ferroelectric phase is accompanied by a transversely modulated spiral magnetic structure.[9] More generally, recent calculations by Katsura and co-workers pointed out a possible microscopic mechanism of the magnetoelectric effect in noncollinear spiral magnets.[10] These studies indicate that a noncollinear spiral spin structure with spin helicity plays a key role in breaking inversion symmetry, i.e., induction of finite electric polarization, in multiferroics. To test this prediction, we focused on a triangular-lattice antiferromagnet, $CuFeO_2$ with the *delafossite* structure (right upper inset of Fig. 1), where various collinear and noncollinear magnetic structures show up by applying magnetic fields. Magnetic, magnetoelectric, and magnetoelastic measurements on $CuFeO_2$ reveal that noncollinear helimagnetic structure plays an essential role in inducing electric polarization. Our results suggest that geometrically frustrated magnetic systems are favorable candidates for magnetoelectric multiferroics.

The most obvious example of a geometrically frustrated magnetic system is a triangular-lattice antiferromagnet (TLA). A typical ordered structure in a TLA is a noncollinear three-sublattice 120° spin configuration where the frustration of the three nearest-neighbor spins on a triangular plaquette is resolved by a 120° rotation of neighboring spins. The ABO_2 family with the delafossite structure[11] (A =nonmagnetic monovalent ion, B=magnetic trivalent ion) has been recently investigated as one of the typical materials for the TLA. Typical magnetic delafossite compounds such as $LiCrO_2$ and $CuCrO_2$ exhibit the 120° spin structure.[2] In contrast, the delafossite $CuFeO_2$ shows a different magnetic structure.[12] Specifically, a collinear commensurate four-sublattice ($\uparrow\uparrow\downarrow\downarrow$) magnetic structure with a wave vector $(q,q,0)$ $(q=1/4)$ is found on each layer in the zero-field ground state, as shown in the left lower inset of Fig. 1 [collinear-commensurate (1/4) phase]. With increasing temperature T, the system shows a sinusoidally amplitude-modulated incommensurate structure at $T_{N2}\sim 11$ K where

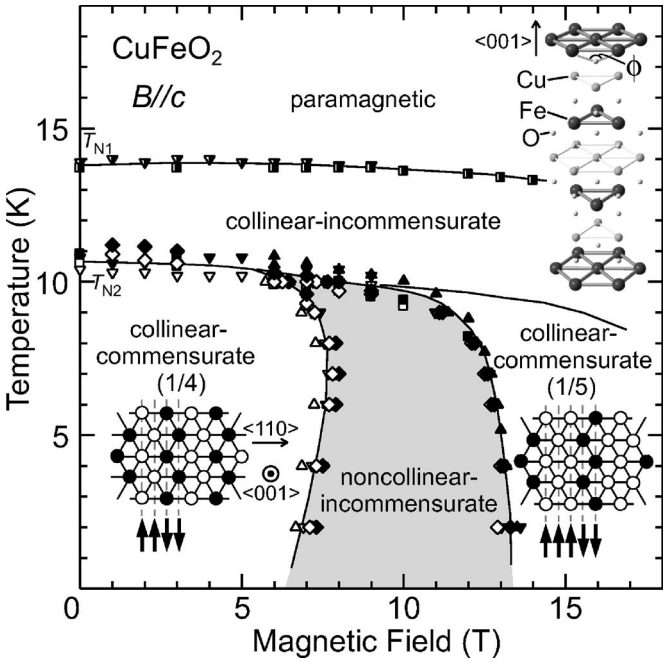

FIG. 1. Temperature (T) versus magnetic field (B) phase diagram of $CuFeO_2$ with B applied along the c axis. Open and filled symbols represent the data points in the cooling (or B-decreasing) and warming (or B-increasing) runs, respectively. Diamond, square, triangle, and inverse triangle data points were obtained by measurements of magnetization, dielectric constant, electric polarization, and magnetostriction, respectively. Upper inset: Crystal structure of $CuFeO_2$. Lower insets: Schematic illustrations of magnetic structures on Fe^{3+} sites at (left) the collinear-commensurate (1/4) and (right) the collinear-commensurate (1/5) states. White and black circles correspond to up and down spin states, respectively. Inversion symmetry is broken at the noncollinear-incommensurate phase (gray area).

 ©2006 The American Physical Society

the magnetic moments are collinearly coupled and the q is T dependent $(\sim 1/4 > q > \sim 1/5)$ (collinear-incommensurate phase), and then becomes paramagnetic at $T_{N1} \sim 14$ K.[13] One of the most intriguing properties of $CuFeO_2$ is the evolution of its magnetic structures, i.e., multistep metamagnetic transitions, when a magnetic field B is applied along the c axis.[14,15] The multistep magnetic phase transitions are ascribed to nearly degenerate spin states around the ground state due to geometrical frustration in this system.

Figure 1 displays the magnetic phase diagram of $CuFeO_2$ as measured by our investigation. Phase boundaries were determined from anomalies in magnetization, dielectric constant, electric polarization, and magnetostriction. It is noteworthy that the phase diagram in Fig. 1 bears a close resemblance to that reported by Mitsuda and co-workers.[16] The application of B between ~ 13 and ~ 20 T induces a collinear-commensurate (1/5) phase ($q=1/5$) where collinear moments along the c axis in each layer exhibit the $(\uparrow\uparrow\uparrow\downarrow\downarrow)$ configuration, as illustrated in the lower right inset of Fig. 1. Between the collinear-commensurate (1/4) and collinear-commensurate (1/5) phases $(\sim 7 < B < \sim 13$ T) there exists another phase (noncollinear-incommensurate phase; gray area in Fig. 1). Although there is no definitive magnetic structure of this phase, neutron diffraction measurements by Mitsuda and co-workers indicate that this phase has an incommensurate complex helical spin structure where the magnetic moments rotate in a helical manner and noncollinearly align along the [110] direction.[16] Here the modulation wave vector is $(q,q,0)$ where q is incommensurate and B dependent $(1/4 > q > 1/5)$. The noncollinear-incommensurate phase will be the focus of this paper. We anticipate the presence of a finite electric polarization at this phase.

Single crystals of $CuFeO_2$ were prepared by a floating zone method, following Ref. 17. Crystals were cut into thin plates with the widest faces parallel and perpendicular to the c axis, and gold electrodes were vacuum deposited onto these faces for measurements of dielectric constant ε and electric polarization P. Dielectric measurements were made at 1 MHz using an *LCR* meter, polarization measurement by the magnetoelectric current with varying magnetic fields. In each measurement, a proper magnetoelectric cooling process was performed to obtain a single ferroelectric domain. The magnetization M and ac susceptibility χ' were measured with a magnetometer. The magnetostriction L was measured using uniaxial strain gauges which were attached to the widest face of the specimens. The contribution of the gauge's magnetoresistance was subtracted after the measurements.

Figure 2(a) displays the T profiles of ac susceptibility parallel $(\chi'_{\parallel})$ and perpendicular $(\chi'_{\perp})$ to the c axis. $\chi'_{\parallel}$ shows a broad maximum at $T_{N1} \sim 14$ K and abruptly drops at $T_{N2} \sim 11$ K on cooling. These anomalies are associated with the transitions from the paramagnetic to collinear-incommensurate phase and the collinear-incommensurate to collinear-commensurate (1/4) phases, respectively. Dielectric constants show that the magnetic phase transitions affect dielectric properties [Fig. 2(b)]. Specifically, a weak T dependence is observed when the electric field is parallel to the c axis $(\varepsilon_{\parallel})$, while distinct anomalies at T_{N1} and T_{N2} are

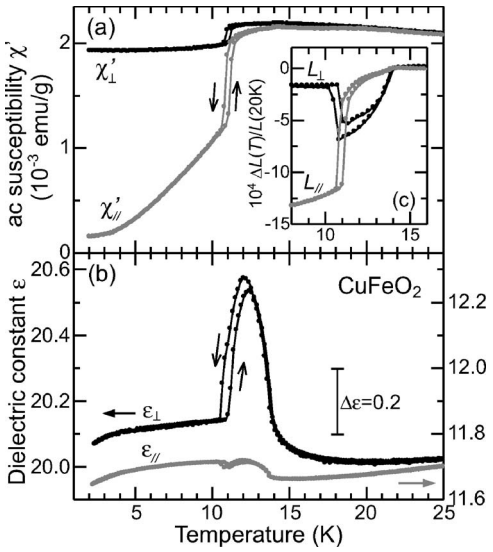

FIG. 2. Temperature profiles of (a) magnetic susceptibility parallel ($\chi_{\parallel}$, gray line) and perpendicular ($\chi_{\perp}$, black line) to the c axis, (b) dielectric constant parallel ($\varepsilon_{\parallel}$, gray line) and perpendicular ($\varepsilon_{\perp}$, black line) to the c axis, and (c) magnetostriction parallel (gray line) and perpendicular (black line) to the c axis in $CuFeO_2$.

clearly seen when the electric field is perpendicular to the c axis $(\varepsilon_{\perp})$.[18] A similar T profile of $\varepsilon_{\parallel}$ around $T_{N1} \sim 14$ K is probably caused by the $\varepsilon_{\perp}$ component due to some misalignment of the sample axis.

It is worth mentioning that the T variation of $\varepsilon_{\parallel}$ at $T_{N2} \sim 11$ K is opposite to that of $\varepsilon_{\perp}$, and cannot be understood in terms of mixing of the $\varepsilon_{\perp}$ component. Presumably the change in sample dimension by the magnetic order, i.e., magnetostriction, can be considered as a possible origin of the opposite T variation at T_{N2}. Figure 2(c) shows the T profiles of the magnetostriction parallel $[L_{\parallel}(T)/L_{\parallel}(20\ \mathrm{K})]$ and perpendicular $[L_{\perp}(T)/L_{\perp}(20\ \mathrm{K})]$ to the c axis. One sees discontinuities at T_{N2} in both directions. The estimated change in $\varepsilon_{\parallel}$ at T_{N2} due to the magnetostriction $(\Delta\varepsilon_{\parallel}/\varepsilon_{\parallel} \sim +1.8 \times 10^{-3})$ is comparable to the measured value $(\sim +1.3 \times 10^{-3})$, indicating that the change in the sample dimension is a result of magnetostriction. The corresponding anomaly in $\varepsilon_{\parallel}$ at T_{N2} can be explained by the magnetostriction. However, the larger change observed in $\varepsilon_{\perp}$ cannot be explained only by the magnetostriction. We also measured the T profiles of the electric polarization by measuring the pyroelectric current. There was no substantial pyroelectric current measured in either direction, showing that the ordered magnetic states at zero magnetic field [collinear-incommensurate and collinear-commensurate (1/4) phases] do not induce inversion-symmetry breaking though the dielectric anomaly.

To further illustrate magnetoelastic coupling, we show the magnetic field profiles of the wave number q of the modulated magnetic structure, magnetization, and magnetostriction parallel $[L_{\parallel}(B)/L_{\parallel}(0\ \mathrm{T})]$ and perpendicular $[L_{\perp}(B)/L_{\perp}(0\ \mathrm{T})]$ to the c axis as a function of $B(\|c)$ at various temperatures in Figs. 3(a)–3(d). We note that the data shown in Fig. 3(a) were taken from Ref. 16. Two magnetization steps are evident at $B \leqslant 14$ T and $T \leqslant 10$ K [Fig. 3(b)]. Comparison between Figs. 3(a) and 3(b) reveals that the first

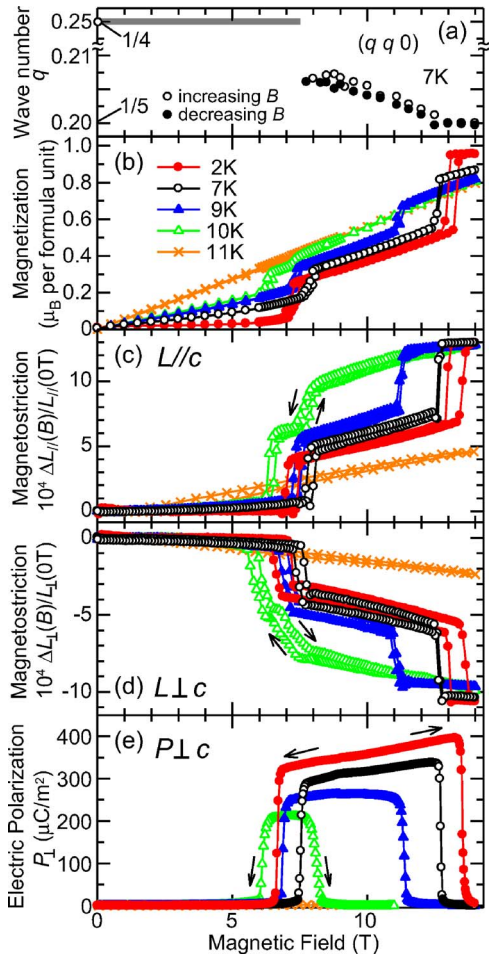

FIG. 3. (Color online) Wave number of modulated magnetic structure (a), magnetization (b), and magnetostriction parallel (c) and perpendicular (d) to the c axis, and electric polarization perpendicular to the c axis (e) of $CuFeO_2$ as a function of magnetic field at selected temperatures. Magnetic field was applied along the c axis. The data of Fig. 3(a) were taken from Ref. 16.

and second steps in the magnetization–magnetic-field curve correspond to the transitions into the noncollinear-incommensurate and the collinear-commensurate (1/5) phases, respectively. We find that the metamagnetic features vanish at 11 K where the collinear-incommensurate state is stabilized.

A comparison of the magnetostriction data [Figs. 3(c) and 3(d)] with those of the magnetization [Fig. 3(b)] reveals an interrelation between the magnetic and magnetoelastic properties. Whereas no remarkable magnetostriction has been observed at 11 K (where the metamagnetic transition does not occur), one sees two discontinuities below 10 K. The onset fields of these two steps coincide with those of the metamagnetic transitions into the noncollinear-incommensurate and the collinear commensurate (1/5) phases. In both steps, $\Delta L_{\parallel}/L_{\parallel}$ abruptly increases while $\Delta L_{\perp}/L_{\perp}$ decreases toward higher-B-induced phases. Therefore, as the system undergoes phase transitions into higher-B phases, the c axis elongates while the ab plane shrinks.

These observations are well described by a change of the nearest-neighbor (NN) Fe-O-Fe bond angle (ϕ) as well as Fe-O length in the delafossite structure (see the right inset of Fig. 1). In the fundamental crystal structure of $CuFeO_2$, ϕ is $\sim 96.7°$ which is rather close to 90°.[11] The Goodenough-Kanamori rules[19–21] suggest that the 180° superexchange d^5-d^5 interaction has strong antiferromagnetic (AF) coupling, and the 90° interaction is either uncertain or weakly AF. The magnetostriction behavior, i.e., the elongation of the c axis and the reduction of the ab plane, may be caused by the decrease of average ϕ. As the system undergoes metamagnetic transitions with increasing B, the ratio of ferromagnetically coupled NN Fe-Fe bonds to the total NN Fe-Fe bonds (f) increases [e.g., $f=1/3$ in the collinear-commensurate (1/4) phase and 7/15 in the collinear-commensurate (1/5) phase]. Energetically it seems that lattice distortion is necessary to reduce the frustration in the TLA.

Figure 3(e) shows the magnetic field dependence of electric polarization with the $E \perp c$ configuration ($P_{\perp}$) at selected temperatures. A comparison of the magnetic field profiles of q and M [Figs. 3(a) and 3(b)] with that of P [Fig. 3(e)] reveals a strong interplay of the evolution of magnetic structure and electric polarization. The data located in the lower-B region of Fig. 3(e) clearly show that P is not induced by B at the collinear-commensurate (1/4) phase. Therefore inversion symmetry is preserved at the collinear-commensurate (1/4) phase. However, $P_{\perp}$ exhibits a sudden increase at the transition field into the noncollinear-incommensurate phase, and becomes finite.[22] The magnitude of $P_{\perp}$ ($\sim 10^2$ $\mu C/m^2$) at the noncollinear-incommensurate phase is comparable to those observed in known multiferroics with long-wavelength magnetic structures.[6–8] With further increase in B, $P_{\perp}$ vanishes again at the transition field into the collinear-commensurate (1/5) phase. It should be emphasized that $P_{\perp}$ becomes finite only at the noncollinear-incommensurate phase but not at the collinear-commensurate and collinear-incommensurate phases. Notably, unlike conventional *improper* ferroelectrics where ferroelectric order emerges at a phase transition from an incommensurate to a commensurate phase,[23] inversion symmetry is broken in an incommensurate phase of $CuFeO_2$. This result provides strong evidence that the noncollinear helical magnetic structure plays a key role in breaking the inversion symmetry of $CuFeO_2$.

To conclude, we now are in a position to speak to the issue of inversion-symmetry breaking in noncollinear helical magnets. The magnetoelectric effect of a helical magnet has been discussed by Siratori and co-workers in the 1980s.[24] In helical magnets, a left-handed or right handed helix is inverted by space inversion I although these two structures never coincide with each other. This can only occur if I is not a symmetry operation; namely, the inversion symmetry is broken in helical magnets, as in ferroelectrics. In helical magnets, the sign of the magnetoelectric coefficient (i.e., the direction of the B-induced electric polarization) can be reversed by changing the sense of the helix. This means that the interaction between two neighboring magnetic moments ($\vec{S}_i$ and $\vec{S}_j$) has to be antisymmetric for the moment exchange. Thus, Siratori and co-workers pointed out that the lowest-order antisymmetric spin coupling, i.e., the Dzyloshinskii-Moriya (DM) interaction $[\vec{D}\cdot(\vec{S}_i \times \vec{S}_j)$, where $\vec{D}$ is the Dzy-

loshinskii vector),[25] plays an important role in the magnetoelectric effect of helical magnets. To understand the operative mechanism of the ferroelectricity in newly discovered multiferroics such as $TbMnO_3$ and $Ni_3V_2O_8$, detailed theoretical treatments for the inversion-symmetry breaking in helical magnets have been undertaken.[8,10,26,27] This collective work indicates a crucial role for the DM interaction and reaches the following expression of the electric polarization: $\vec{P} \propto \vec{e}_{ij} \times (\vec{S}_i \times \vec{S}_j)$, where $\vec{e}_{ij}$ is the unit vector connecting the sites i and j. This indicates that a finite electric polarization can appear if (a) the magnetic moments at the sites i and j are coupled noncollinearly in a helical manner, and (b) the spin rotation axis $[\parallel(\vec{S}_i \times \vec{S}_j)]$ does not coincide with the modulation wave vector of the helix $[\parallel \vec{e}_{ij}]$. The direction of P is perpendicular to the spin rotation axis and the wave vector of the helix, and can be reversed by the exchange of the two moments, i.e., the change of the sense of the helix. In the present case of $CuFeO_2$, finite electric polarization appears only at the noncollinear-incommensurate helical phase, which validates the extension of the helical (or spiral) mechanism to $CuFeO_2$. Although a detailed magnetic structure of the noncollinear incommensurate phase of $CuFeO_2$ is lacking at present, investigation of the electric polarization could lead to insight into magnetic structures in noncollinear helical magnets.

In summary, we investigated the magnetic, magnetoelectric, and magnetoelastic properties of a triangular-lattice antiferromagnet $CuFeO_2$ showing magnetic-field-induced collinear-noncollinear magnetic phase transitions. The present study demonstrates that geometrically frustrated magnetic systems that often favor noncollinear magnetic structures are promising candidates for multiferroics with strong magnetoelectric interaction.

We gratefully acknowledge discussions with R. Kajimoto, F. Ye, Y. Ren, and G. Lawes, and thank J.L. Sarrao and K.J. McCllelan for help with experiments. This work was supported by the U.S. DOE.

[1] A. P. Ramirez, Annu. Rev. Mater. Sci. **24**, 453 (1994).
[2] M. F. Collins and O. A. Petrenko, Can. J. Phys. **75**, 605 (1997).
[3] N. A. Hill, J. Phys. Chem. B **104**, 6694 (2000).
[4] M. Fiebig, J. Phys. D **38**, R123 (2005).
[5] T. Kato, K. Machida, T. Ishii, K. Iio, and T. Mitsui, Phys. Rev. B **50**, R13039 (1994).
[6] A. Inomata and K. Kohn, J. Phys.: Condens. Matter **8**, 2673 (1996).
[7] T. Kimura, T. Goto, H. Shintani, K. Ishizaka, T. Arima, and Y. Tokura, Nature (London) **426**, 55 (2003).
[8] G. Lawes, A. B. Harris, T. Kimura, N. Rogado, R. J. Cava, A. Aharony, O. Entin-Wohlman, T. Yildrim, M. Kenzelmann, C. Broholm, and A. P. Ramirez, Phys. Rev. Lett. **95**, 087205 (2005).
[9] M. Kenzelmann, A. B. Harris, S. Jonas, C. Broholm, J. Schefer, S. B. Kim, C. L. Zhang, S.-W. Cheong, O. P. Vajk, and J. W. Lynn, Phys. Rev. Lett. **95**, 087206 (2005).
[10] H. Katsura, N. Nagaosa, and A. V. Balatsky, Phys. Rev. Lett. **95**, 057205 (2005).
[11] C. T. Prewitt, R. D. Shannon, and D. B. Rogers, Inorg. Chem. **10**, 791 (1971).
[12] S. Mitsuda, H. Yoshizawa, N. Yamaguchi, and M. Mekata, J. Phys. Soc. Jpn. **60**, 1885 (1991).
[13] S. Mitsuda, N. Kasahara, T. Uno, and M. Mase, J. Phys. Soc. Jpn. **67**, 4026 (1998).
[14] Y. Ajiro, T. Asano, T. Takagi, M. Mekata, H. A. Katori, and T. Goto, Physica B **201**, 71 (1994).
[15] O. A. Petrenko, M. R. Lees, G. Balakrishnan, S. de Brion, and G. Chouteau, J. Phys.: Condens. Matter **17**, 2741 (2005).
[16] S. Mitsuda, M. Mase, K. Prokes, H. Kitazawa, and H. A. Katori, J. Phys. Soc. Jpn. **69**, 3513 (2000).
[17] T. R. Zhao, M. Hasegawa, and H. Takei, J. Cryst. Growth **166**, 408 (1996).
[18] We measured the dielectric constant along both the [110] and the $[1\bar{1}0]$ directions, but did not observe any substantial difference.
[19] J. Kanamori, J. Phys. Chem. Solids **10**, 87 (1959).
[20] J. B. Goodenough, *Magnetism and the Chemical Bond* (Interscience, New York, 1963).
[21] P. W. Anderson, in *Magnetism I*, edited by G. Rado and H. Shuhl (Academic Press, New York, 1963), Chapter 2.
[22] We confirmed the sign reversal of $P_\perp$ by reversing poling electric fields. We also measured $P_\parallel$ in magnetic fields, but $P_\parallel$ is by an order of magnitude smaller than $P_\perp$, which may be caused by $P_\perp$ component due to some misalignment of sample axes.
[23] R. Blinc and A. P. Levanyuk, *Incommensurate Phases in Dielectrics 1. Fundamentals* (North-Holland, Amsterdam, 1986).
[24] K. Siratori, J. Akimitsu, E. Kita, and M. Nishi, J. Phys. Soc. Jpn. **48**, 1111 (1980); K. Siratori and E. Kita, *ibid.* **48**, 1443 (1980).
[25] I. Dzyloshinskii, J. Phys. Chem. Solids **4**, 241 (1958); T. Moriya, Phys. Rev. **120**, 91 (1960).
[26] I. A. Sergienko and E. Dagotto, Phys. Rev. B **73**, 094434 (2006).
[27] M. Mostovoy, Phys. Rev. Lett. **96**, 067601 (2006).